2010 21st International Lightning Detection Conference
19 – 20 April • Orlando, Florida, USA
3rd International Lightning Meteorology Conference
21 – 22 April • Orlando, Florida, USA

A SIMULATION OF ELECTRIFICATION AND LIGHTNING IN A SUPERCELL STORM USING ENKF TO ASSIMILATE DOPPLER RADAR OBSERVATIONS

Kristin M. Kuhlman
Cooperative Institute for Mesoscale Meteorological Studies, University of Oklahoma and
NOAA/National Severe Storms Laboratory, Norman, OK, USA

Don MacGorman, Edward R. Mansell, Conrad Ziegler
NOAA/National Severe Storms Laboratory, Norman, OK, USA

Michael Biggerstaff
School of Meteorology, University of Oklahoma, Norman, OK, USA

1. Introduction

On 29 May 2004, a line of convective cells formed along a dryline near Elk City, OK; one intensified to a heavy-precipitation (HP) supercell north of Weatherford, OK as it moved into the TELEX domain (MacGorman et al. 2008). The data set established through this field campaign provides an excellent opportunity for using Ensemble Kalman Filter (EnKF) assimilation of radar data to produce a storm simulation having characteristics similar to those of the observed storm, so that we can examine hypotheses concerning the storm's electrification and lightning.
During the TELEX campaign, the storm was observed by two C-band mobile radars providing rapid, high resolution volume scans, two S-band 88D radars, the National Lightning Detection Network (NLDN), the Oklahoma Lightning Mapping Array (LMA), and mobile electric field meter soundings through the storm, with additional soundings of the storm environment acquired by Vaisala GPS radiosondes. These observational platforms documented the storm for over three hours, capturing the mature stage of the storm, including two F2 tornadoes near Geary, OK. The availability of nearly continuous mobile Doppler radar data from SR2 on 29 May during the intense period as it moved through the TELEX domain provides high-resolution (time and space) data for assimilation.

2. Data and Methodology

2.1 Observational Data

Lightning activity, both in-cloud and cloud-to-ground, can give insight into storm charge structure. The main tools used to investigate the observed lightning in this study are the Oklahoma Lightning Mapping Array (LMA) and the National Lightning Detection Network (NLDN). This data is used as a basis for comparison with the electrification and lightning of the simulated storm.

This study primarily utilizes data from one of the two Shared Mobile Atmospheric Research and Teaching (SMART) radars (Biggerstaff et al. 2005) that observed the storm for over two hours as it passed through central OK. The SMART radars (SR1 and SR2) completed volume scans of the storm every three minutes, with sector volume scans of approximately 120 degrees used for both radars. Elevation angles ranged from 0.5 - 33.5 degrees with increments of 0.3 - 3.0 degrees. Prior to the assimilation process, SR data were edited to subjectively remove ground blockage, velocity and range folding, and regions of high noise.

2.2 Model Details

The Collaborative Model for Multiscale Atmospheric Simulation (COMMAS) is used to complete the simulations. COMMAS is a three-dimensional, nonhydrostatic model which uses the basic equation set from Klemp and Wilhelmson (1978) with prognastic equations for momentum, pressure, potential temperature, and turbulent kinetic energy (Coniglio et al. 2006). This study utilizes a double-moment microphysics scheme that predicts hydrometeor number concentration and mass for six hydrometeor types: cloud droplets, rain, cloud ice, snow, graupel and hail (Mansell et al 2010).

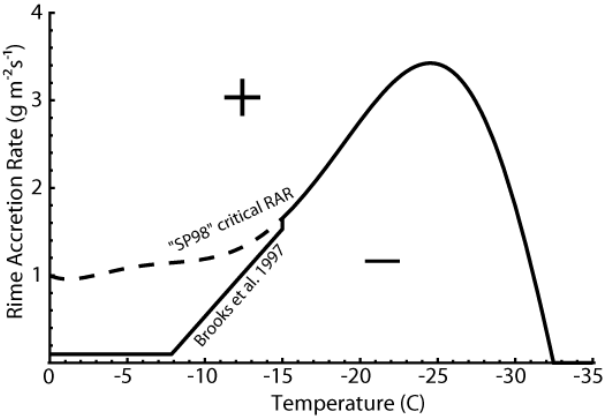

Figure 2.1: Noninductive charge separation sign-reversal curve. The critical rime accretion rate (RAR) curve follows (Saunders and Peck 1998) for T < −15 C (shown as dashed curve for T > −15 C) and Brooks et al. (1997) at warmer temperatures. Charge transfer is set to zero for T < −33 C. Adapted from Mansell et al. (2010).

Following the sensitivity tests of Mansell et al. (2005) and Kuhlman et al. (2006), electrification in the model is composed primarily of noninductive charging using the Saunders and Peck (1998) laboratory results with an adjustment for warmer temperatures following Brooks et al. (1997) (Fig. 2.1).

Charge is conserved within the model domain. A charge density is connected with every hydrometeor type. As mass shifts between categories in the microphysics, the charge also is transferred from one category to another (e.g. mass from ice to rain). Small ion processes are also included in the model (Mansell et al. 2003) with conservation equations defined for both positive and negative ion concentrations.

Lightning flashes are parameterized by a stochastic dielectric breakdown model as described in Mansell et al. (2002, 2005). The lightning develops bidirectionally across a uniform grid with each step chosen randomly from among the surrounding points at which the electric field meets or exceeds a threshold value for propagation. After each step, the electric field is calculated to determine the contribution by the lightning channel. The end result is a branched or fractal-like leader structure of each flash in three dimensions.

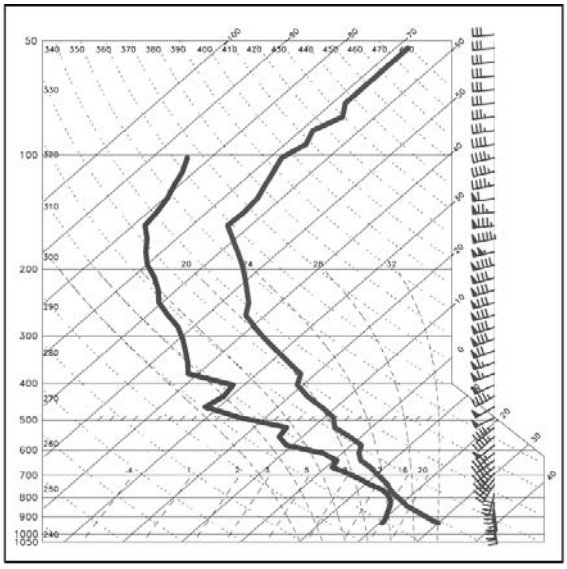

Figure 2.2: Skew T-log p diagram for the base state in the assimilation experiment interpolated to model grid levels. Below 400 mb, the sounding is taken from an environmental sounding released near Weatherford, OK. Above 400 mb, the sounding is from data from the National Weather Service Norman, OK sounding released at 0000 UTC. Wind barbs (flags) represent 10 m/s (50 m/s).

2.3 Simulation and EnKF set-up

The model domain is 140 km x 140 km x 22 km with 1 km grid spacing in the horizontal and vertical grid spacing of 200 m stretched to a maximum of 500 m at 20 km over 53 grid points. The domain is initialized to be horizontally homogeneous using a combination of two soundings merged into one (Fig. 2.2). Below 400 mb, the sounding is taken from an environmental sounding released near Weatherford, OK. Above 400 mb, the sounding is from data from the National Weather Service Norman, OK

sounding released at 0000 UTC.

A 24-member ensemble is used for the simulations. Each member is initiated using randomly perturbed (4 K) warm bubbles inserted in the boundary layer where cells are indicated by regions of radar reflectivity. The ensemble members require some spin up time, which allows for some comparison of precipitation initiation in the various microphysics schemes. Reflectivity and velocity from SR2 are assimilated in approximately five-minute intervals from 2320 UTC to 0040 UTC up to 8.5km in height.

Before assimilation, each sweep of SR2 data was objectively analyzed separately to grid points on the conical scan surfaces following Dowell et al. (2004) and Dowell and Wicker (2009). A Cressman objective analysis is used with grid points spaced 2000 m apart in the horizontal direction using a radius of influence of 1000 m. The EnKF methodology used to assimilate the observations follows the process described by Dowell and Wicker (2009). All the members assimilate the same observations, but to keep them independent, random perturbations are added to the observations assimilated in each member. In short, the entire assimilation process is completed by converting each model state to an expected observation, comparing the value with the observation and observational error distribution, determining the incremental difference and creating the state variable increments, and finally advancing the model and repeating the steps at the next observational time.

Electrification processes are not included for the first 40 min of the simulations. After a "mature" storm is produced, electrification is turned on in the first four members as well as the ensemble mean. Electrification is limited to these members due to the high computation cost of the electrification and lightning parameterizations.

3. Results

The simulated precipitation and wind fields of the ensemble were similar to those of the observed storm, as one would expect. Generally, for all members of the ensemble, there are weaker reflectivity values in the simulations when compared to corresponding dual-Doppler analyses (Fig. 3.1). The ensemble mean low-level mesoscyclone was considerably weaker than the dual-Doppler derived mesocyclone, as also shown by Ziegler et al. (2009), though the location and shape are similar (Fig. 3.1, middle). The vertical velocity values of the main updraft in the simulations were slightly smaller at low-levels, but nearly identical at mid and upper levels of the storm.

At the start of the electrification process (40-55 min into the simulation), the main updraft area consists of a normal polarity tripole structure with a main negative charge region, an upper positive and smaller lower negative region. By 60-70 min into the simulations, the charge structure is much more involved as charged hydrometeors move further away from the updraft core, lightning activity dissipates pockets of charge, and other charged particles are recycled through the updraft. As such, the charge structure is quite complex, more involved than can be described by a dipole or tripole structure.

In the region of the main updraft, there is typically very little charge below 4 km, however, above this height through storm top there is quite often 5 or 6 different charge layers, all with small horizontal extent. In the downdraft, frequently 6 to 7 different charge layers are seen and these tend to be of much longer horizontal extent, extending away from region of active charging in the main updraft.

At low levels (below 4 km), the RFD and hook echo region consists of positive charge throughout the simulation. Correspondingly, the CG flashes that do occur here are all of negative polarity. CG activity is more active in the FFD area of the storm, where regions of both negative and positive charge are present in the lowest layer at different times with both +CG and –CG flashes occurring, though infrequently. As seen in previous studies, the model continues to greatly under-predict CG flashes relative to observations (Fig. 3.2).

The total flash rates of the simulations are consistent with the extremely high values of the observed storm (Fig. 3.2). Throughout the analyzed period flash rates remained above 200 per min for the storm and at times peaked above 400-600 flashes per min (the first peak that occurs

at the beginning of the analyzed period between 2345-2355 UTC occurs just after electrification

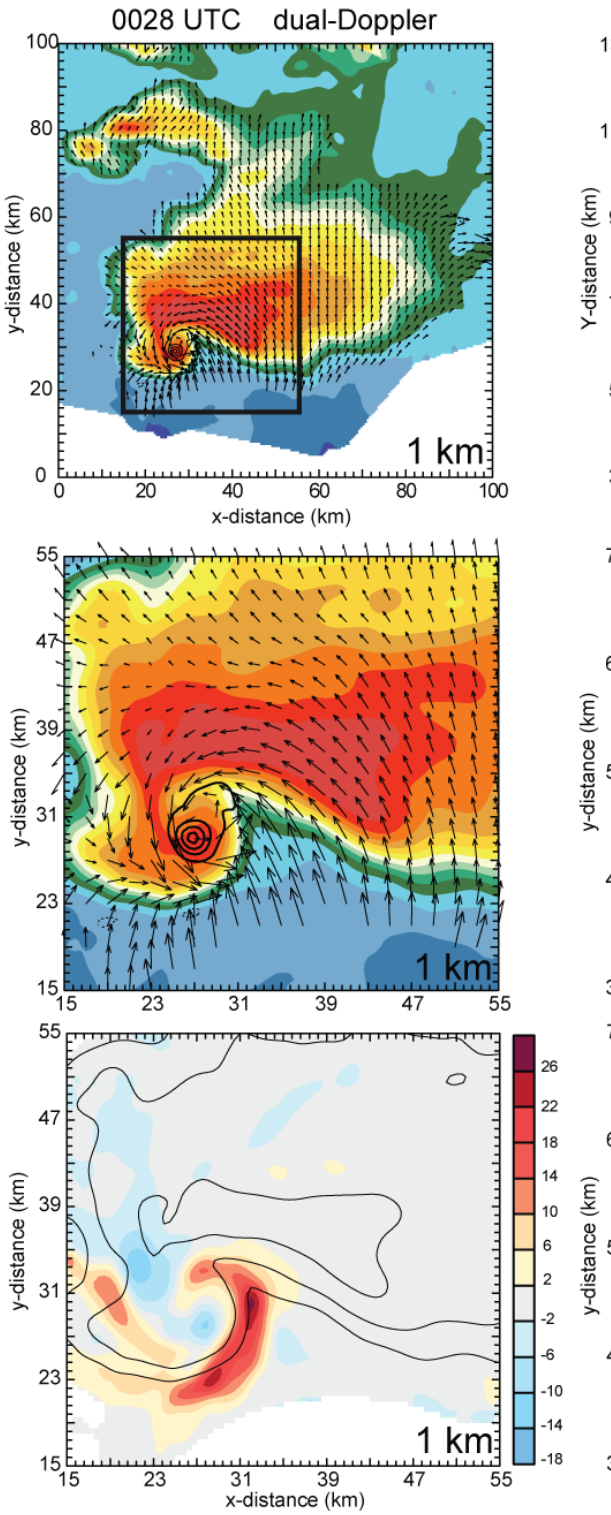

Figure 3.1: (top) Reflectivity and wind vecto
Doppler analysis (left) and member 1 of simu
shown in top panels, reflectivity, wind vectors
10×10^-3 s−1, beginning at 10×10−3 s-1. (bo
contours of reflectivity every 20 dBZ.

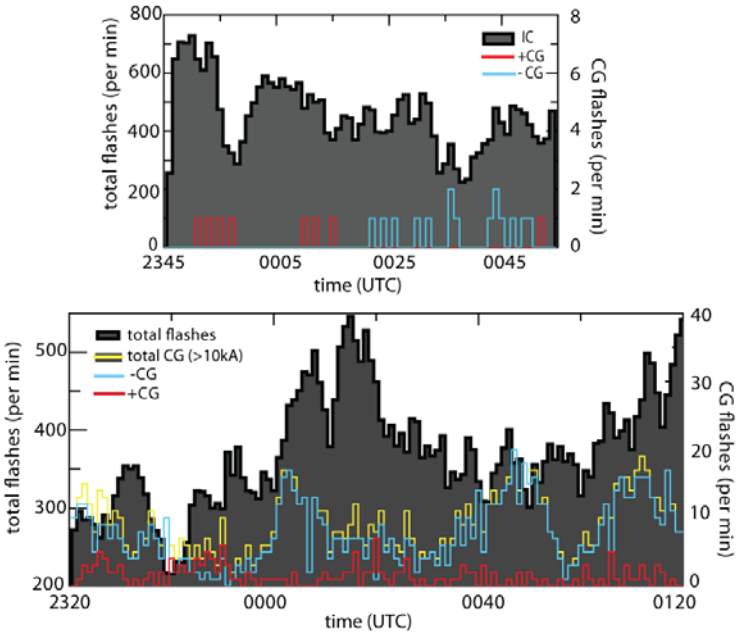

Figure 3.2: Flash rate for the member 1 of the simulations (top) and the observed storm (bottom), panels are aligned by time (UTC). Total flash rate rate in gray fill (left axis) and CG flash rate (right axis) red (positive) and blue (negative). Observations from LMA (total) and

was first started so the early values are likely a bit inflated). Flash rates of this magnitude, above 400-600 flashes per min, are not necessarily common for the parameterization during simulations of other supercell storms. This particular storm had much higher concentrations of graupel and hail, allowing for higher charging rates than in previous supercell simulations where the maximum flash rate is closer to 200 flashes per min with mean levels around 75 flashes per min (Kuhlman et al. 2006).

The graupel/hail within the updraft region acquires either positive and negative charge dependent upon the specific conditions. At warmer temperatures (greater than -20 C) and higher liquid water contents, the larger ice hydrometeors gained positive charge, while on the periphery of the updrafts at lower liquid water contents strong negative charging is active. Outside the core of the storm there is very little active charging. Infrequently, secondary areas of active charging occur in the FFD area. This secondary charging region is only active when there is a higher concentration of cloud water available in combination with the presence of high graupel concentrations. The charging in this region contributes to a brief increase in lightning in the area, but no charge from here or even the continuous stronger charging in the updraft core makes its way into the anvil. Charge on particles out of updraft region either descend quickly into the FFD or are neutralized by lightning flashes and are not advected into the anvil region. Unlike the observed storm (Kuhlman et al. 2009), the simulations contained absolutely no anvil lightning. We hypothesize that some other electrification mechanism, possibly such as a non-inductive ice-ice mechanism operating under conditions of ice supersaturation in low liquid water content (e.g., Mitzeva et al. 2005), may be necessary to produce charge and lightning in these regions.

Even though reflectivity values between 5 and 7 km are consistently between 30 and 50 dBZ on SE side of the storm there is very little to no lightning below 7 km in this location. This is representative of the lack of charged particles in this region. Charging rates on this side of the main updraft core are much lower to near nonexistent when compared to northwest of the main updraft and extending downshear to the northeast. This area seems to be lacking on the higher concentrations of water vapor and cloud ice that are present on the northwest side, thus dampening the charging rate. Similarly, the observations also show a lack of LMA activity between 6-9 km on southern side of storm (although it is not completely absent as seems to be the case with the simulations). Above 9 km there is an increase of charge and lightning activity, though the majority of the initiations still occur on the north and northeast side of the core.

A transient lightning hole is present in all electrified members of the simulations. The lightning hole also appears at similar timing within the different members, in less than 2-3 time steps of each other. However, some members do depict larger and more persistent holes than other members. A lightning hole type feature first appears around 2355-0003 UTC in a couple of the members, with another short lived one appearing around 0015-0023 in almost all the

electrified members. The feature isn't seen again until 0038 UTC in member 1 and then appears again in all the members around 0048-0054 UTC after data is no longer being assimilated.

Member 1 replicates the lightning hole near end of simulation 0049-0052. The location matches well with the BWER (on SE edge) and the main updraft area (Fig. 3.3), similar to what was seen in the dual-Doppler and LMA analysis (not shown). The charge density in this area, while not absent, also appears to be weaker during this time frame than in time steps not containing a lightning hole. There is also a complete absence of charge and active NI charging below 8 km through the region where the updraft is greater than 40 ms^{-1} (Fig. 3.3). The central region of the lightning hole is almost completely lacking large ice particles, as hail mixing ratios are below 2 g kg^{-1} in the center of the hole.

Lightning occasionally does initiate between at 13-15 km above the main updraft region and following the cloud boundary directly down shear from this region. It appears that the lightning in this region is most commonly initiated between opposite polarity charge advected from the updraft core, however at times the lightning does seem to be initiated between the cloud charge and the screening layer charge enhanced at the cloud boundary.

Overall, the simulated lightning flash rates were very large, as was observed, and the distribution of charge in the main body of the storm was similar to that inferred from lightning observations. The simulation produced observed lightning holes, though not as frequently as the observations. The simulations also replicated some of the lightning in the region of the overshooting top, though failed to produce the observed lightning initiations (or even lightning channels) in the distant downstream anvil. Instead, the simulated lightning was confined to the main body of the storm.

4. References

Biggerstaff, M. I., L. J. Wicker, J. Guynes, C. L. Ziegler, J. M. Straka, E. N. Rasmussen, A. Doggett, L. D. Carey, J. L. Schroeder, and C. Weiss, 2005: The Shared Mobile Atmospheric Research and Teaching radar: A collaboration to enhance research and teaching. Bull. Amer. Meteor. Soc., 86, 1263–1274.

Brooks, I. M., C. P. R. Saunders, R. P. Mitzeva, and S. L. Peck, 1997: The effect on thunderstorm charging of the rate of rime accretion by graupel. Atmos. Res., 43, 277–295.

Coniglio, M. C., D. J. Stensrud, and L. J. Wicker, 2006: Effects of upper-level shear on the structure and maintenance of strong quasi-linear mesoscale convective systems. J. Atmos. Sci., 63, 1231–1252.

Dowell, D. C. and L. J. Wicker, 2009: Additive noise for storm-scale ensemble data assimilation. J. Atmos. Oceanic Tech., 26, 911–927.

Dowell, D. C., F. Zhang, L. J. Wicker, C. Synder, and N. A. Crook, 2004: Wind and temperature retrievals in the 17 May 1981 Arcadia, Oklahoma, supercell: Ensemble Kalman filter experiments. Mon. Wea. Rev., 132, 1982–2005.

Klemp, J. B. and R. B. Wilhelmson, 1978: Simulations of right- and left-moving storms produced through storm splitting. J. Atmos. Sci., 35, 1097–1110.

Kuhlman, K. M., C. L. Zielger, E. R. Mansell, D. R. MacGorman, and J. M. Straka, 2006: Numerically simulated electrification and lightning of the 29 June 2000 STEPS supercell storm. Mon. Wea. Rev., 134, 2734–2757.

Kuhlman, K. M., D. R. MacGorman, M. I. Biggerstaff, and P. R. Krehbiel, 2009: Lightning initiation in the anvils of two supercell storms. *Geophys. Res. Lett.*, *36*(7). doi: 10.1029/2008GL036650.

MacGorman, D. R., W. D. Rust, T. Schuur, M. E. Biggerstaff, J. Straka, C. L. Ziegler, E. R. Mansell, E. C. Bruning, K. M. Kuhlman, N. Lund, J. Helsdon, L. Carrey, K. Eack, W. H. Beasley, P. R. Krehbiel, and W. Rison, 2008: TELEX: The thunderstorm electrification and lightning experiment. Bull. Amer. Meteor. Soc., 89, 9971013.

Mansell, E. R., D. R. MacGorman, C. L. Ziegler, and J. M. Straka, 2002: Simulated three-dimensional branched lightning in a numerical thunderstorm model. J. Geophys. Res., 107, 2–1.

— 2005: Charge structure and lightning sensitivity in a simulated multicell thunderstorm. J. Geophys. Res., 110.

Mansell, E. R., C. L. Ziegler, and E. C. Bruning, 2010: Simulated electrification of a small thunderstorm with two-moment bulk microphysics. J. Atmos. Sci., 67. 171-194, DOI: 10.1175/2009JAS2965.1.

Mitzeva, R.P., Saunders, C.P.R., Tsenova, B., 2005. A modeling study of the effect of cloud saturation and particle growth rates on charge transfer in thunderstorm electrification. Atmos. Res. 76, 206–221.

Saunders, C. P. R. and S. L. Peck, 1998: Laboratory studies of the influence of the rime accretion rate on charge transfer during crystal/graupel collisions. J. Geophys. Res., 103, 13949–13956.

Ziegler, C., L. Wicker, M. Biggerstaff, D. Betten, E. Mansell, K. Kuhlman, and D. MacGorman: Evolution of downdraft thermodynamics and low-level rotation in the tornadic 29 May 2004 Geary, OK, USA supercell storm. Preprints, 5th Euro. Conf. on Severe Storms, Landshut, Germany, 2 pp.

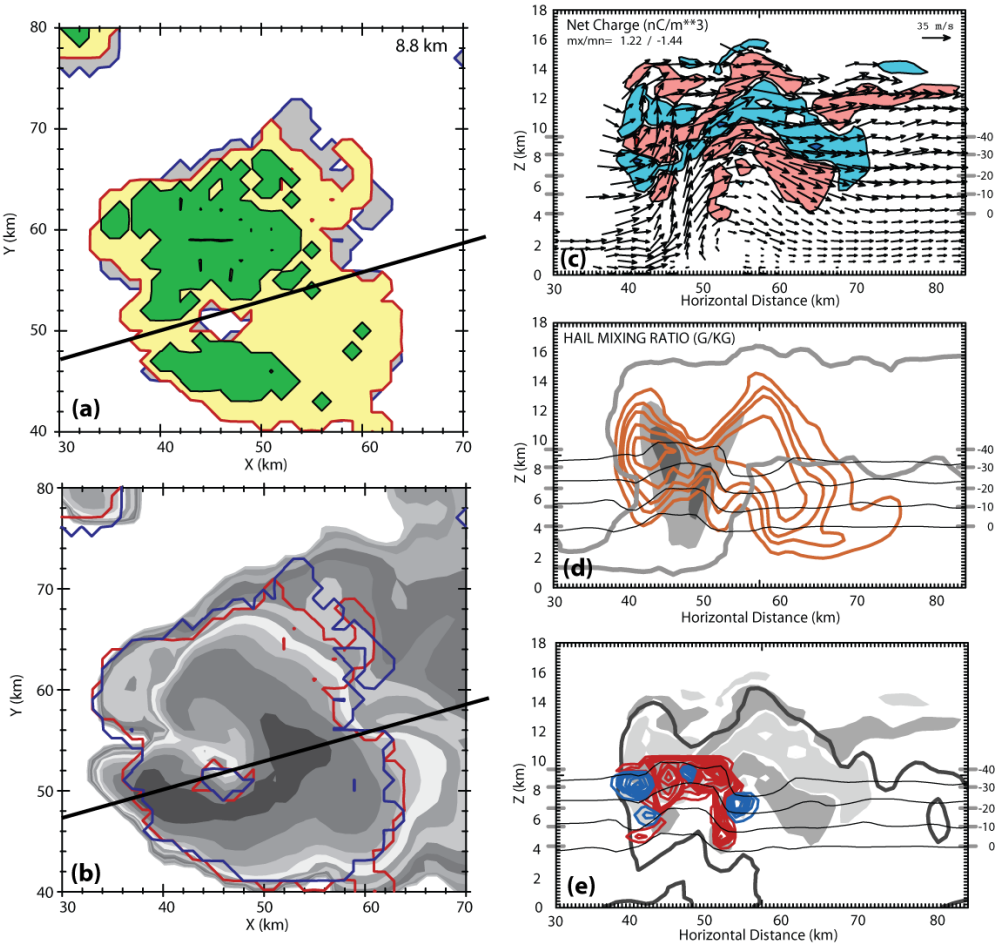

Figure 3.3: Lightning hole at 0050 UTC in member 1 of simulation. (a) Composite of lightning initiations (green), positive leaders (yellow fill, red contour), and negative leaders (gray fill, blue contour) within 2.5km from 8.8km. (b) Reflectivity at 8.8km (grayscale) with positive (red) and negative (blue) leaders contoured. (c) Net Charge density, positive (red) and negative (blue) and wind vectors. (d) Contours of hail mixing ratio(orange), cloud outline (gray) and grayfill of vertical velocity at 25 and 40 m/s. (e) Contours of noninductive charging rate of graupel/hail (positive (red) and negative (blue)) and 20 dBZ reflectivity (dark gray). Grayfill of negative (light) and positive (dark) charge density.